



Properties of nanofibrillated cellulose from different raw materials and its reinforcement potential

Tanja Zimmermann*, Nicolae Bordeanu, Esther Strub

Empa, Swiss Federal Laboratories for Materials Testing and Research, Wood Laboratory, Ueberlandstrasse 129, CH-8600 Dübendorf, Switzerland

ARTICLE INFO

Article history:

Received 2 October 2009

Accepted 16 October 2009

Available online 22 October 2009

Keywords:

Electron microscopy
Atomic force microscopy
Tensile testing
Intrinsic viscosity
Nanofibrillated cellulose
Nanocomposites

ABSTRACT

Five commercial wood and wheat straw fiber sources with different morphologies were mechanically disintegrated into nanofibrillated cellulose (NFC). The processing times for disintegration varied, depending on the sizes and the moisture content of the starting materials. A decrease in polymerization degree (DP) for the fibrillated materials between 15% and 63% could be observed. Nevertheless, all isolated NFC materials showed homogenous network structures. They were used for the production of composite films with hydroxypropyl cellulose (HPC) as matrix and different proportions of NFC and two commercial fibrillar-fibrous celluloses as reinforcing components. Films with the commercial, more inhomogeneous fibrillated celluloses showed up to 2.5 times lower strength and up to four times lower stiffness. It appeared that homogeneity of the NFC material is more important for its reinforcement potential than the DP. A proper pre-treatment and choice of starting cellulose materials can reduce energy consumption, a key issue for industrial up-scaling.

© 2009 Elsevier Ltd. All rights reserved.

1. Introduction

With a total quantity on earth of 10^{11} tons (Coughlan, 1985), cellulose is the most abundant, renewable and biodegradable natural polymer (Mathew, Chakraborty, Oksman, & Sain, 2006). In lignocellulosic fibers that have diameters in the micrometer and lengths in the millimeter range cellulose acts as a structural element with a content of approximately 45%. The cellulose is organized as aggregates of fibrils embedded in the matrix substance lignin. One single cellulose fibril is approx. 3–4 nm thick and several tens of micrometers long and consists of crystalline parts linked to amorphous domains. The cellulose chains are stabilized laterally by hydrogen bonds between hydroxyl groups (Fengel & Wegener, 1989). The isolation of cellulose fibril aggregates from wood pulp has first been described by Turbak, Snyder, and Sandberg (1983). Recently, nano-sized cellulose fibril aggregates could be successfully isolated from fibers in high quality by using high-shear homogenization or refining processes (Iwamoto, Nakagaito, & Yano, 2007; Zimmermann, Pöhler, & Geiger, 2004).

Due to the crystalline parts of cellulose fibrils, they have extraordinary mechanical properties, interesting for various applications. The modulus of elasticity along the chain axis (MOE) of the perfect crystal of native cellulose has been calculated by different authors using X-ray diffraction or Raman spectroscopy (Gillis, 1970; Sakurada, Nukushina, & Ito, 1962; Tashiro & Kobayashi,

1991) and was estimated between 130 GPa up to 250 GPa. Cellulose fibrils have due to their amorphous regions lower mechanical properties. Hsieh, Yano, Nogi, & Eichhorn, 2008, e.g. calculated 114 GPa for the MOE of single bacterial cellulose filaments using a Raman spectroscopic technique. However, the reinforcement potential of cellulose fibrils for (bio)polymers has been shown in many studies, e.g. Zimmermann et al., 2004; Nakagaito & Yano, 2005; Iwatake, Nogi, & Yano, 2008. Beside outstanding mechanical properties, cellulose fibrils have other advantages like biocompatibility, transparency and high reactivity due to the presence of hydroxyl groups at their large surface.

The terminology for cellulose fibrils is not consistent, often the terms microfibrillated cellulose, e.g. Herrick, 1984, cellulose nanofibrils or cellulose nanofibers, e.g. Yano et al., 2005; Dalmás, Chazeau, Gauthier, Cavaille, & Dendievel 2006 are used. As the nano-sized material (target diameters below 100 nm) is obtained by a fibrillation procedure the term nanofibrillated cellulose (NFC) will be used in this study.

In the last decade there has been a growing interest from industry to use nano-sized cellulose, especially for polymer applications in packaging, biomedicine, adhesives, fibers, electronics and automotive. The potential for these applications has been shown and discussed in various publications (Haugaard et al. 2001; Pandey et al., 2005; Wan, Hutter, Millon, & Guhados, 2006; Yano et al. 2005). A comprehensive overview is given in the review paper of Hubbe, Rojas, Lucia, & Sain, 2008.

Several industrial cellulose fiber producers aim at an up-scaling of NFC isolation and some fibrillar-fibrous products are already

* Corresponding author. Tel.: +41 44 823 43 89; fax: +41 44 823 40 07.
E-mail address: tanja.zimmermann@empa.ch (T. Zimmermann).

available on the European market. However, until now, to the knowledge of the authors, there is only one Japanese product (Celish) in homogenous fibrillation quality on the market (Daicel Chemical Industries). Important for industrial producer is the interrelationship between the cellulose raw material used, the processing and the quality of the final fibrillated products. An indication for the mechanical performance potential might be the chain lengths and aspect ratios of the celluloses (Battista, 1975, chap. 2), assessable by determination of the degree of polymerization (DP).

The objective of our investigations was to separate nanofibrillated cellulose (NFC) at the greatest possible lengths and diameters below 100 nm from different starting cellulose materials with methods also capable for a later industrial up-scaling. Furthermore, the suitability of the obtained NFC as well as two commercial fibrillar-fibrous cellulose products for the reinforcement of polymers was determined by tensile testing. A special attention was given to measurements of the intrinsic viscosity of all cellulose materials and the calculation of the DPs. The fibril alignment in reinforced polymer films was analyzed by TEM and AFM.

2. Experimental

2.1. Materials

2.1.1. Starting cellulose materials for nanofibrillated cellulose (NFC) isolation in the laboratory

Nanofibrillated cellulose (NFC) was isolated from different commercial raw materials such as:

- Softwood sulfite pulp (SSP) of spruce (*Picea abies*) and white fir (*Abies alba*), Borregaard Schweiz AG, Switzerland.
- Wheat straw (*Triticum sp.*) pulp (WSP1), University of Natural Resources and Applied Life Sciences, Austria.
- Refined fibrous wheat straw cellulose suspension (WSP2), Vitacel, J. Rettenmaier & Söhne GmbH & Co. KG, Germany.
- Refined beech wood (*Fagus sylvatica*) pulp powder (BWP1), Mikro-Technik GmbH & Co. KG, Germany.
- Refined fibrous beech wood pulp suspension (BWP2), Arbocel, J. Rettenmaier & Söhne GmbH & Co. KG, Germany.

The characteristics of all starting cellulose materials like form, dimensions, moisture content, Kappa Number and Hemicelluloses content are summarized in Table 1.

2.2. Isolation of nanofibrillated cellulose (NFC)

2.2.1. Mechanical pre-treatment

For isolation of NFC five commercially available cellulose materials have been used (see above and in Table 1).

Mechanical pre-treatment of cellulose materials was conducted with lab-scale equipment (Fig. 1) composed of a 10 liter thermostatic reactor coupled to an inline dispersing (ILD) system (Mega-tron MT 3000, Kinematica AG, Switzerland).

Prior to mechanical pre-treatment, the dry sulfite and wheat straw pulp were milled in order to reduce their fiber dimensions

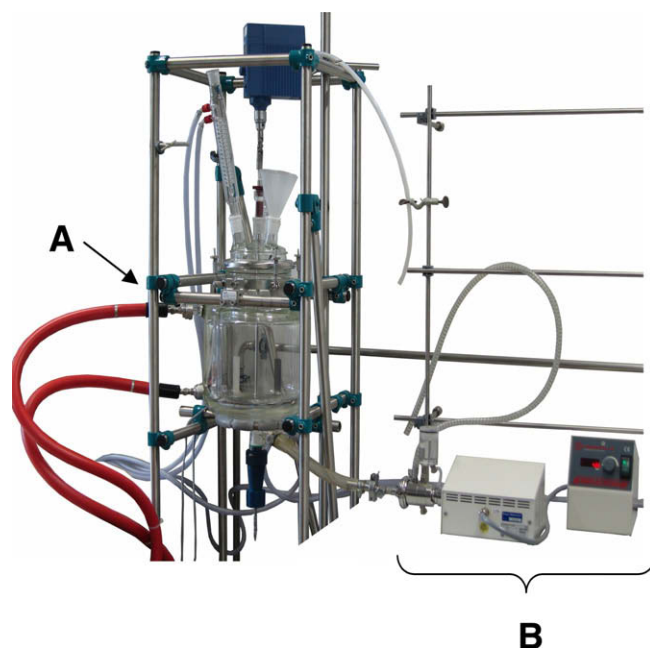


Fig. 1. Lab-scale equipment for the mechanical pre-treatment of cellulosic raw materials. (A) Ten liter reactor for suspending cellulose raw material in water. (B) Inline dispersing system (ILD) for the extraction of cellulose fibril bundles from the cell wall of the raw materials with concomitant pre-dispersion.

(L and D) and to improve their swelling capacity in water. The cellulose materials were added in the reactor into 8 liter of deionized water. The resulting mixtures were cooled to 15 °C and treated with the ILD at 20,000 rpm in order to divide the pulp fibers into smaller parts, defined as *cellulose fibril bundles* (CFB). Homogeneous CFB suspensions in water were obtained after different processing times depending on the cellulose material used. Table 2 compiles all parameters required for each cellulose material in order to get a homogeneous aqueous CFB suspension which is suitable for the following high-shear disintegration and homogenization.

2.2.2. Mechanical high-shear disintegration and homogenization

The method, first described in Zimmermann et al., 2004, consists of a solely mechanical treatment under high pressure that separates the nanofibrillated cellulose from the aqueous CFB suspensions by high shearing-stress generated in the interaction chambers of a *Microfluidizer® High-Shear Processor* (Microfluidics Corporation, USA) during processing (Fig. 2).

The mechanical high-shear disintegration and homogenization comprises in subjecting the aqueous CFB suspensions at high pressure (up to 1500 bar) to a certain number of passes through the interaction chambers (Y- and Z-type geometry, diameters between 75 and 200 µm) of a lab-scale *Microfluidizer* type M-110Y. Pre-treated CFB suspensions can be diluted prior to the disintegration and homogenization step if necessary due to increase in viscosity. Concentration range and number of passes through the interaction

Table 1
Characteristics of starting materials.

Celluloses	Morphology	Diameter	Length	Moisture content (%)	Kappa number	Hemicellulose content (%)
Softwood sulfite pulp (SSP)	Fiber sheets	µm-scale (5–70 µm)	>1 mm	6.3	0.8	10.92
Wheat straw pulp (WSP1)	Fiber sheets	µm-scale (3–90 µm)	>1 mm	6.6	0.6	20.98
Wheat straw pulp (WSP2)	Refined fibers, never dried	nm/µm-scale (50 nm–8 µm)	>2 µm	95	3.2	14.02
Beech wood pulp (BWP1)	Pulp powder, particles	µm-scale (3–70 µm)	<200 µm	8.5	0.8	8.55
Beech wood pulp (BWP2)	Refined fibers, never dried	nm/µm-scale (50 nm–8 µm)	>2 µm	90	1.0	7.07

Table 2

Processing parameters for the mechanical pre-treatment of cellulose materials.

Raw material	Milling [s]	Maximal Concentration [% (w/w)]	Processing time ILD [min]
Softwood sulfite pulp (SSP)	25	1.5	320
Wheat straw pulp (WSP1)	15	2.5	300
Wheat straw pulp (WSP2)	–	3.0	30
Beech wood pulp (BWP1)	–	8.0	60
Beech wood pulp (BWP2)	–	2.0	60

Table 3

Processing parameters for mechanical high-shear isolation of nanofibrillated cellulose from aqueous CFB suspensions of different cellulose raw materials.

Aqueous CFB suspension	Number of passes at 1500 bar	Concentration range [% (w/w)]
Softwood sulfite pulp (SSP)	7	0.5–0.8
Wheat straw pulp (WSP1)	7	0.5–1.5
Wheat straw pulp (WSP2)	6	0.5–2.0
Beech wood pulp (BWP1)	4	1.0–6.0
Beech wood pulp (BWP2)	6	1.0–2.0

2.4. Degree of polymerization (DP)

The limiting viscosity number of all cellulose materials was determined after ISO 5351 (Anonymus, 2004a).

The different starting cellulose materials and the nanofibrillated celluloses isolated thereof were dried for 24 h at a temperature of 50 °C. A defined portion of cellulose was dissolved in a cupri-ethylenediamine (CED) solution. From the CED and testing solutions (starting materials as well as nanofibrillated cellulose samples) the running time through a marked distance of a capillary-tube viscometer was determined. From the running times and the defined cellulose portions, the limiting viscosity number $[\eta]$ of each testing sample was calculated using the Schulz–Blaschke formula (Anonymus, 2004a). The average degree of polymerization of the nanofibrillated cellulose samples was calculated from $[\eta]$ using the Staudinger–Mark–Houwink equation (Gruber & Gruber, 1981).

2.5. Microscopy

2.5.1. Field emission scanning electron microscopy (FE-SEM)

For the preparation of samples for FE-SEM (Jeol 6300F, Jeol Ltd., Japan) investigations, glimmer plates were fixed with a conducting carbon on specimen holder. A drop of a diluted and stirred aqueous cellulose fiber (starting materials) or NFC (disintegrated materials) suspension (1:10 v/v) was placed on the glimmer plates. The samples were sputtered directly with a platinum layer of about 5 nm (BAL-TEC MED 020 modular high vacuum coating systems, BAL-TEC AG, Principality of Liechtenstein). SEM images were recorded with an accelerating voltage of 5 kV and a working distance of 39 mm.

2.6. Preparation of nanocomposite films

Nanocomposite films out of the polymer *hydroxypropyl cellulose* (HPC, Mw = 1,000,000, low viscosity; Sigma–Aldrich Chemie GmbH, Germany) and NFC from all cellulose materials as well as the two commercial fibrous products WSP2 and BWP2 were cast. The other starting cellulose materials with bigger fiber dimensions could not be used for the production of films.

First, a 5% (w/w) solution of HPC was prepared by adding dry HPC in deionized water and stirring the mixture at 60 °C until a clear solution was obtained. Increasing amounts of the aqueous nanofibrillated cellulose suspensions (1, 5, 10 and 20% (w/w)) were added to the HPC solution and blended with an Ultra-Turrax (Type T25 basic, IKA-Werke GmbH & Co. KG, Germany) two times for 30 s, respectively. The obtained suspensions were degassed prior to casting in silicone forms and dried at standardized conditions (23 °C/65% relative humidity).

2.7. Tensile tests

Specimens were stamped out of the nanocomposite films according to EN ISO 527-4 (Anonymus, 1997). Universal tensile tests were carried out using a Zwick Z010 universal testing machine

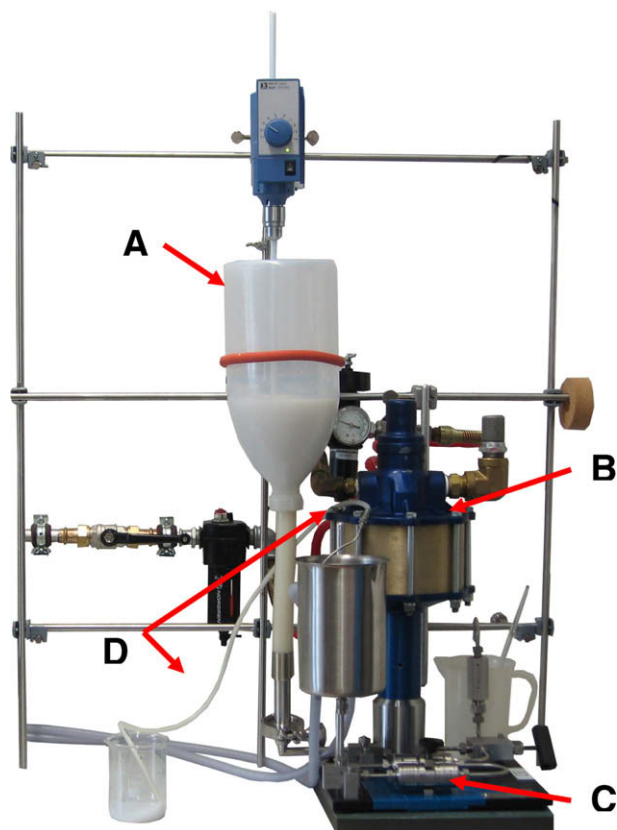


Fig. 2. Microfluidizer lab-scale high-shear processor type M-110 Y for isolation of nanofibrillated cellulose by mechanical disintegration and homogenization of aqueous CFB suspensions. (A) Container for the CFB suspension equipped with stirrer. (B) Air pump for the generation of high processing pressure (up to 1500 bar). (C) Patented interaction chambers (Y- and Z-type). (D) Cooling loop and product outlet.

chambers of the *Microfluidizer* are listed in Table 3 for the CFB suspension of each cellulose material.

2.3. Chemical analysis

The Kappa numbers of the five starting celluloses were determined by measuring the consumption of potassium permanganate according to ISO 302 (Anonymus, 2004b). The residual lignin of the samples can be estimated by multiplying the Kappa number with a factor of 0.15.

Other samples of the same celluloses were submitted to total hydrolysis with sulfuric acid, the hydrolysed carbohydrates were separated by borate complex ion exchange chromatography, and detected photometrically with copper-2,2-bicinchonate reagent according to Uremovic et al. (1994).

(Zwick GmbH & Co. KG, Germany) with a 200 N load cell. The tests were carried out at 20 °C/65% relative humidity with a loading speed of 10 mm/min. Strain was appointed by using an optical strain gauge. Modulus of elasticity (MOE) was calculated with the software *testXpert* (version V11.0, Zwick GmbH & Co. KG, Germany) from the slope of the linear region in the stress–strain diagrams.

2.8. Microscopy

2.8.1. Transmission electron microscopy (TEM)

Small extracts ($2 \times 2 \text{ mm}^2$) of the HPC/NFC nanocomposites containing 20% (w/w) nanofibrillated cellulose were embedded after Spurr, 1969 and stained with uranyl acetate. Ultra thin sections (approx. 60 nm thick) of the transverse film surfaces were sectioned using an ultramicrotome fitted with a diamond knife. The sections were mounted on Formvar coated grids and examined with a transmission electron microscope (Philips CM200, The Netherlands) at an accelerating voltage of 120 kV.

2.8.2. Atomic force microscopy (AFM)

Small pieces ($5 \times 5 \text{ mm}^2$) of the HPC nanocomposite films (the smoother lower side of the films on top) containing 20% (w/w) nanofibrillated cellulose were glued (Superglue, Turbo Klebstofftechnik GmbH, Switzerland) onto aluminium sample holders and examined with a NanoSurf Mobile S AFM (Nanosurf AG, Switzerland) using Tapping Mode™. The surface was cleaned with pressurized air. Images were taken in height mode, where the deflection of the cantilever is directly used to measure the *z* position, and in phase mode, where the phase shift of the cantilever is used to determine differences in material constitution.

3. Results and discussion

3.1. Characteristics of starting cellulose materials

Table 1 gives an overview of the characteristics of the five softwood, hardwood or wheat straw cellulose materials used for the isolation of nanofibrillated cellulose (NFC). Images of the celluloses are provided in Fig. 3a–e (left side). Two of the cellulose materials are dried pulp fibers (SSP and WSP1) with diameters in the μm -range (3–90 μm) and lengths clearly in millimeter scale. BWP 1 is a dry pulp powder where the fibers are distinctly reduced in length (<200 μm) compared with SSP and WSP1. The two fibrous refined and never dried fiber products (WSP2 and BWP2) partly show a fibrillar structure (Figs. 3c and e, left). However, the fibrillation appears not homogeneous. Thus, fine fibrillar structures with diameters clearly in the nanometer range as well as bigger cellulose fibril aggregates or fiber parts with micrometer dimensions are visible.

The Kappa number of all celluloses is between 0.6 and 1 and only for the fibrous wheat straw cellulose WSP2 higher with a value of 3.2. The results point to low concentrations of rest lignin (<1%) for all celluloses. The Kappa number is an indication of the lignin content of pulp and is determined by the consumption of permanganate (ISO 302, 2004b). However, there is no general and unambiguous relationship between the Kappa number and the lignin content of pulp. The relationship varies according to the wood species and delignification procedure during pulping. Other compounds than lignin oxidized by KMnO_4 like hexen uronic acid will increase its consumption, and therefore the Kappa number (Gellerstedt, Li, & Sevastyanova 2000). The two wheat straw celluloses (WSP1 and WSP2) with a striking difference in Kappa Number were purchased from different suppliers. It is possible that the bleaching treatment was different for both celluloses. Bleach-

ing with chlorine or chlorine dioxide in contrast to peroxide e.g. dissolves more or less completely hexen uronic acid. It is possible that a higher content of hexen uronic acid led to different Kappa numbers.

The highest hemicellulose contents could be found for WSP1 and WSP2 (20.98% and 14.02%, respectively). Panthapulakkal, Zereschian, & Sain 2005 determined hemicellulose contents in the same range (18.59%) for mechanically processed wheat straw fibers.

3.2. Isolation of nanofibrillated cellulose

The aim of the mechanical pre-treatment is to minimize the size of the cellulose fibers to cellulose fibril bundles (CFB) in such a way that the resulting still inhomogeneous suspension can pass the high pressure homogenizer without causing a clogging of its interaction chambers. Typical CFB have diameters between 200 and 800 nm. Generally, a good pre-treatment reduces the passes through the high-shear homogenizer (Microfluidizer), necessary for an optimal fibrillation of the material.

The morphology and dimensions of the starting celluloses determined the times necessary for mechanical pre-treatment and high-shear homogenization. The celluloses WSP2, BWP1 and BWP2 with smaller dimensions (reduced in lengths and diameters, Table 1) needed a shorter processing time through the inline dispersing system and less passes through the high-shear homogenizer (Tables 2 and 3). Especially BWP1 (provided in powder form) needed only four passes through the homogenizer when compared to the dry pulps SSP and WSP1 with seven passes (Table 3). The use of never dried and therefore swollen (not hornified) cellulose as starting material (WSP2, BSP2) shortened the time necessary for the pre-treatment. An influence of the hemicellulose or lignin content on the processing time could not be derived from the results of the chemical analysis (Table 1).

The decision to stop the disintegration process was done by visual evaluation: During processing, the viscosity of the cellulose suspension increased continuously. The disintegration process was stopped when a high increase in viscosity could be observed and no solid residue could be detected anymore when rubbing the suspension between two fingers.

Fig. 3a–e, right shows network structures of nanofibrillated cellulose out of all wood and wheat straw celluloses. Mechanical disintegration and homogenization through the Microfluidizer resulted in fibril structures with diameters predominantly below 100 nm and estimated lengths in the micrometer range. This is in accordance to other researchers who used similar homogenization processes (Leitner, Hinterstoisser, Wastyn, Keckes, & Gindl, 2007). Due to the high density of hydroxyl groups at their surfaces (Fengel & Wegener, 1989), the fibrils strongly interacted by hydrogen bonds. Thus, it was not possible to determine the exact lengths of the fibrils. The laboratory fibrillated materials showed a more homogeneous network structure compared to the two refined commercial fibrous celluloses (Fig. 3c and e).

Shearing stresses to the longitudinal fiber axis (caused by the homogenization process, pressure up to 1500 bar, interaction chambers with Y or Z morphology and sizes between 200 and 75 μm), disintegration time and passes through the homogenizer are considered as influencing parameters for the resulting fibril dimensions. This is also supported by other studies. Bruce, Hobson, Farrent, & Hepworth, 2005 used a food homogenizer where a cellulose suspension was pressurized to 500 bars and passed through a minute gap in a homogenizing valve. They obtained some separation of fibrils (demonstrated by electron micrographs) but had still many cell wall fragments within the resulting suspension. Thus, the pressure was probably not high enough to generate an optimal shear stress when material passed the gap. Nakagaito &

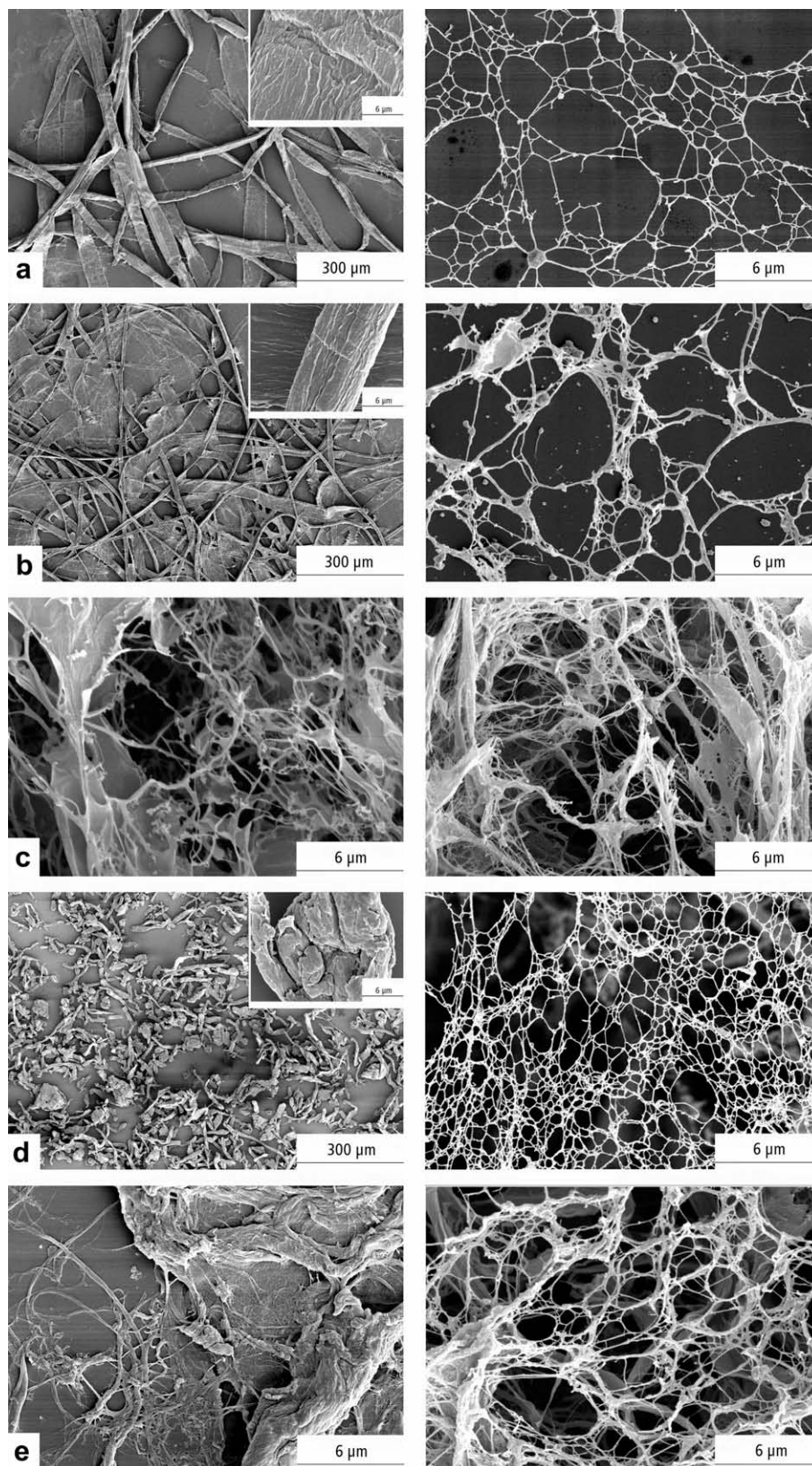


Fig. 3. FE-SEM micrographs: On the left side commercial cellulose starting materials: softwood sulfite pulp fibers (a), wheat straw pulp fibers (b), refined fibrillar-fibrous wheat straw pulp (c), refined beech wood pulp powder (d), refined fibrillar-fibrous beech wood pulp (e). On the right side mechanically, laboratory isolated nanofibrillated cellulose out of the stated starting materials.

Yano, 2004 obtained the best fibrillation results for wood fibers after 30 passes through a refiner and 30 passes through a homogenizer. They demonstrated the homogenization of the cellulose material during processing by a sequence of SEM images. The results are comparable with our fibrillation results after 30–320 min through the Inline-Disperser and 4–7 passes through the high pressure homogenizer (Tables 2 and 3). Leitner et al., 2007 needed 10–15 passes at 300 bar through a homogenizer to obtain cellulose fibrils at nanoscale, thus about twice as much as we needed at higher pressures in our study (Table 3). As the preparation for SEM, especially the drying, might influence the appearance of the visible network structures (e.g. occurrence of film building, reagglomerations or hornification) it is difficult to detect a possible influence of rest lignin and hemicellulose content on the fibrillation result.

The most important issue when thinking about an up-scaling of the nanofibrillated cellulose production in Industry is the energy consumption. In our process, the length of the mechanical pre-treatment has not a big impact when calculating energy consumption for NFC production. The Inline Dispersing System needs 185 Wh (measured with a galvanometer) when it is run with 20,000 rpm (maximum power). The Microfluidizer (high pressure shear processor) needs 8.5 kWh (manufacturer's data) assuming a processing pressure of 1500 bar (compare experimental section). 10 l cellulose suspension with a concentration of 1–2 wt.% needs about 15 min to pass once the Microfluidizer. The number of passes needed through the Microfluidizer is therefore crucial for the energy consumption of the process (e.g. 14.875 kW for SSP, 8.5 kW for BWP1).

Recently, several researchers focus on the development of less energy consuming disintegration methods using enzymatic or chemical pre-treatment. Abe, Iwamoto, & Yano, 2007, e.g. succeeded in the production of NFC out of wood powder with only one pass through a grinder. SEM images show a striking homogeneous network of nanofibrillated cellulose with a filament width of 15 nm. However, they applied a severe chemical pre-treatment. Henriksson, Berglund, Isaksson, Lindström, & Nishino, 2008 used cellulase enzymes to favour attack on the amorphous regions of the cellulose and therefore to facilitate the separation of the material into homogeneous nanofibrillated cellulose by high pressure homogenization. For an industrial up-scaling it will be necessary to find optimal parameters of chemical and mechanical treatments for isolation of NFC to lower consumption of energy and chemicals.

3.3. Degree of polymerization (DP)

The viscosity has often been determined as indirect measurement of the average fiber length of pulps, resp. the degradation due to chemical or mechanical treatment (Lapierre, Bouchard, & Berry, 2006). It is generally found that strength properties decrease with decreasing DP of the cellulose. Thus, the DP might be a tool for evaluation of the performance of NFC as reinforcing component in various matrices.

Table 4 shows the intrinsic viscosity as well as the calculated degree of polymerization (DP) of the raw and fibrillated cellulose materials. The highest viscosities could be measured for the pulps. The viscosity of the refined commercial fibrous beech wood pulp product was very low (120 ml/g). Fibrillation in the laboratory led to a decrease in viscosities/DPs between 15% and 63%. The drop is higher for starting materials with a high viscosity; materials that are already degraded due to chemical/mechanical pre-treatment (as the commercial fibrous products) show lower decreases. The viscosities of the fibrillated materials are between 100 and 390 ml/g. After Battista, 1975, chap. 2, the DP strongly correlates with the aspect ratio of the fibrils. This means, shorter fibrils with constant diameter have a lower DP. However, assuming that the

Table 4

Intrinsic viscosity and degree of polymerization of all cellulose materials.

Cellulose material	Intrinsic viscosity η (ml/g)	Degree of polymerization (DP)
Softwood sulfite pulp (SSP)	800	2249
SSP fibrillated	350	825
Wheat straw pulp (WSP1)	570	1433
WSP1 fibrillated	320	749
Wheat straw pulp (WSP2)	441 [*]	1025 [*]
WSP2 fibrillated	280	674
Beech wood pulp (BWP1)	460	1088
BWP1 fibrillated	390	930
Beech wood pulp (BWP2)	120	291
BWP2 fibrillated	100	230

^{*} Measurements on cellulose of new batch as the original material was degraded by micro organisms.

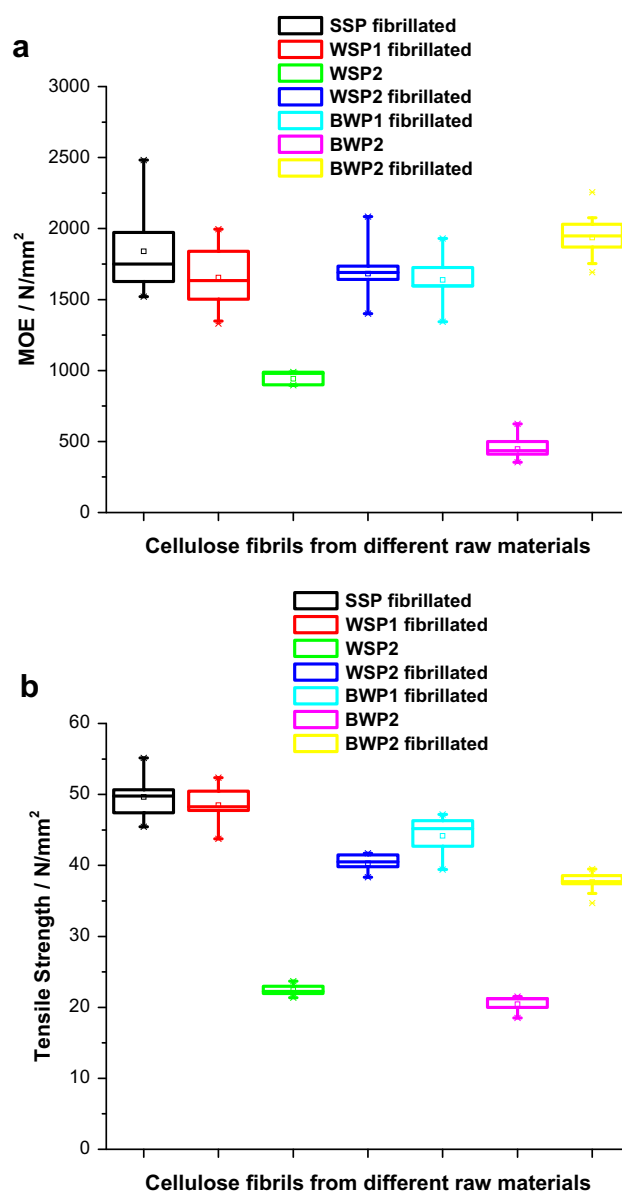


Fig. 4. (a) Modulus of Elasticity (MOE) and (b) tensile strength of films out of laboratory isolated cellulose and commercially available fibrous cellulose materials (Table 3) in HPC. The fibril content of the films is 20% (w/w). MOE of neat HPC 393 N/mm², Tensile strength 8.4 N/mm².

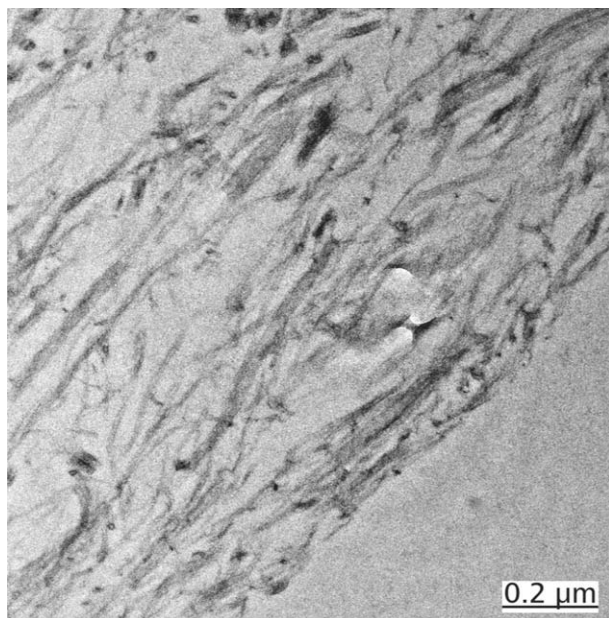


Fig. 5. TEM micrograph: Transverse section of a HPC/NFC film embedded in epoxy resin (after Spurr) with a fibril content of 20% (w/w). The fibrils (from sulfite pulp, SSP) are dispersed within the polymer and show an aligned structure perpendicular to the cutting direction.

NFC with lower DP contains shorter fibrils, these differences had no impact on the mechanical performance as reinforcing component in the HPC composites (compare paragraph below). Important might be the network forming capability. All laboratory isolated celluloses formed stable network structures (Fig. 3, right) independent from the calculated DP and had fibrils with diameters still in the micrometer range.

3.4. Mechanical properties of cellulose nanocomposites

As the two commercial fibrous starting cellulose materials (WSP2 and BWP2) partly show a fibrillar structure (Fig. 3c and e, left), they could be used for the production of composite films. These films achieved an up to four times lower MOE and an up to 2.5 lower tensile strength compared to films with laboratory fibrillated cellulose (Fig. 4a and b). This fits well to the results obtained by SEM (compare Fig. 3). The commercial WSP2 and BWP2 were less homogeneous, showed bigger aggregates and partly no network formation. Thus, a homogenous fibrillation of NFC is very

important for a good reinforcing effect. This has also been described by Nakagaito & Yano (2004) who evaluated how the degree of fibrillation of pulp fibers affects the mechanical properties of cellulose/phenol resin composites. They found that fibrillation solely on the surface of the fibers is not effective in improving composite strength. At a distinct point in the fibrillation stage they observed an abrupt increase in the mechanical properties of the composites.

All laboratory fibrillated materials showed MOE and tensile strengths on a high level compared to the commercial fibrous products. The highest stiffness was obtained for the fibrillated commercial product BWP2, although the calculated DP was lower than for all other celluloses. The tensile strength of this cellulose was slightly lower, especially when compared with NFC from sulfite or wheat straw pulp. However, also the tensile strength of the fibrillated BWP1 had a slightly lower performance, although this cellulose showed the highest DP of all fibrillated materials.

Network formation of nano-sized cellulose as well as the stability of such networks has been proposed to be of great importance for high reinforcement efficiency (Dufresne, Cavaille, & Helbert, 1997; Hajji, Cavaille, Favier, Gauthier, & Vigier, 1996; Helbert, Cavaille, & Dufresne 1996). Taking into account the results of the viscosity measurements, it is assumed that a homogeneous fibrillation is more important for the mechanical performance than the polymerization degree of the cellulose. A good distribution of network forming NFC probably ensures the stress transfer from the HPC matrix to the fibrils upon loading.

3.5. Morphology of cellulose nanocomposites

Despite the difficulties to obtain TEM and AFM images in high quality, the fibril dispersion within the polymer matrix could be observed for the HPC composite film loaded with 20% (w/w) of laboratory isolated NFC from sulfite pulp (Fig. 5). Only a few agglomerations are visible, besides the NFC is well dispersed. This is in accordance to the results of Zimmermann, Pöhler, & Schwaller, 2005 showing a good distribution of NFC within the same polymer. The TEM results were confirmed by AFM for the same composite (Fig. 6). On the AFM images, the fibril network within the HPC matrix seems to be very dense, thus the fibrils are building a large surface area and are probably wrapped by the polymer.

4. Conclusions

Cellulose fibrils with diameters below 100 nm and lengths in the micrometer range could be isolated out of different raw materials by mechanical dispersion and high pressure (up to

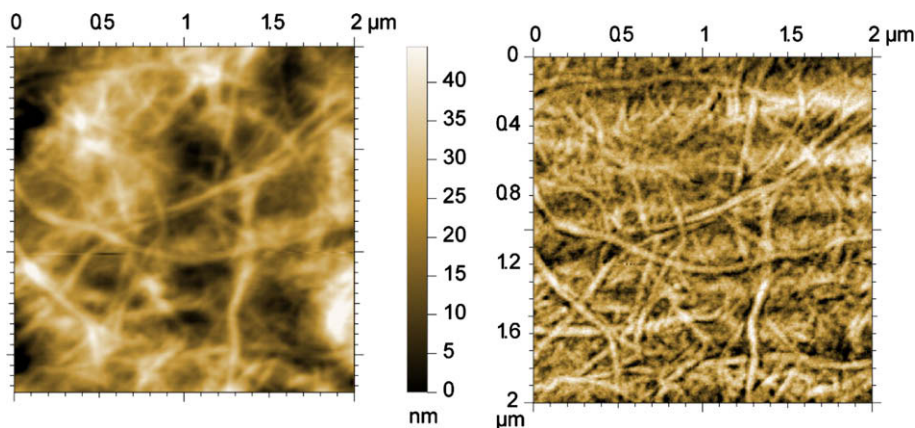


Fig. 6. AFM topographic (left) and phase image (right) of fibrillated sulfite pulp (SSP) in HPC (20% w/w). The fibrils are randomly arranged and show a dense structure. The polymer portion is not distinguishable. It is reasonable that the fibrils are wrapped by the polymer.

1500 bar) homogenization processes. The treatment resulted in nano-scaled fibril networks. Two commercial fibrous celluloses showed bigger cellulose aggregates with micrometer dimensions and a less homogeneous network structure.

The degree of polymerization of the NFC materials used, had no obvious impact on the mechanical properties of the hydroxypropyl cellulose (HPC) composites. Much more important for the reinforcement potential was the quality of fibrillation. Thus, the tensile strength of HPC films with lab-fibrillated cellulose is up to 2.5 and the MOE up to four times higher compared to films reinforced with the commercial fibrous celluloses.

A problem in industry is the energy consumption during the isolation process of NFC which has a direct influence on the eco friendliness and the processing costs. A quantitative method to assess the fibrillation quality during processing will be important for NFC producer. According to this study, the polymerization degree gives no sufficient indication for the reinforcement potential of the NFC material. The microscopic methods used, allow only a qualitative assessment of the disintegration process. Therefore, the aim of further studies will be the development of a suitable quality control.

Acknowledgements

Thanks are due to Anja Fischer for TEM characterization, Monika Graf for AFM measurements and Christian Eyholzer who gave support concerning the viscosity measurements. The support of the VTI-Institute for Wood Technology and Biology, University of Hamburg (D) concerning the chemical analysis of the celluloses is gratefully acknowledged. We are also grateful to Philippe Tinguet and Klaus Richter for carefully reading the manuscript.

References

- Abe, K., Iwamoto, S., & Yano, H. (2007). Obtaining cellulose nanofibers with a uniform width of 15 nm from wood. *Biomacromolecules*, 8, 3276–3278.
- Anonymus. (1997). Plastics-determination of tensile properties – Part 4: Test conditions for isotropic and orthotropic fibre-reinforced plastic composites. ISO 527-4.
- Anonymus. (2004a). Pulps-determination of limiting viscosity number in cupri-ethylenediamine (CED) solution. ISO 5351.
- Anonymus. (2004b). Pulps-determination of kappa number. ISO 302.
- Battista, O. A. (1975). *Microcrystal polymer science*. New York: McGraw-Hill.
- Bruce, D. M., Hobson, R. N., Farrent, J. W., & Hepworth, D. G. (2005). High-performance composites from low-cost plant primary cell walls. *Composites Part A – Applied Science and Manufacturing*, 36, 1486–1493.
- Coughlan, M. P. (1985). Cellulose hydrolysis – The potential, the problems and relevant research at the galway. *Biochemical Society Transactions*, 13, 405–406.
- Dalmas, F., Chazeau, L., Gauthier, C., Cavaille, J. Y., & Dendievel, R. (2006). Large deformation mechanical behaviour of flexible nanofiber filled polymer nanocomposites. *Polymer*, 47, 2802–2812.
- Dufresne, A., Cavaille, J. Y., & Helbert, W. (1997). Thermoplastic nanocomposites filled with wheat straw cellulose whiskers. *Polymer Composites*, 18, 198–210.
- Fengel, D., & Wegener, G. (1989). *Wood – Chemistry, ultrastructure, reactions*. Berlin, New York: Walter de Gruyter.
- Gellerstedt, G., Li, J., & Sevastyanova, O. (2000). The relationship between kappa number and oxidizable structures in bleached kraft pulps. *Proceedings of the international pulp bleaching conference* (Vol. 1, pp. 203–206). Halifax.
- Gillis, P. P. (1970). The elastic constants of cellulose. *Cellulose Chemistry Technology*, 4, 123–135.
- Gruber, E., & Gruber, R. (1981). Viskosimetrische Bestimmung des Polymerisationsgrades von Cellulose. *Das Papier*, 35, 133–141.
- Hajji, P., Cavaille, J. Y., Favier, V., Gauthier, C., & Vigier, G. (1996). Tensile behavior of nanocomposites from latex and cellulose whiskers. *Polymer Composites*, 17, 612–619.
- Haugaard, V. K., Udsen, A. M., Mortensen, G., Hoegh, L., Petersen, K., & Monahan, F. (2001). Potential food applications of biobased materials. *Starch-Stärke*, 53, 189–200.
- Helbert, W., Cavaille, J. Y., & Dufresne, A. (1996). Thermoplastic nanocomposites filled with wheat straw cellulose whiskers. 1. Processing and mechanical behaviour. *Polymer Composites*, 17, 604–611.
- Henriksson, M., Berglund, L. A., Isaksson, P., Lindström, T., & Nishino, T. (2008). Cellulose nanopaper structures of high toughness. *Biomacromolecules*, 9, 1579–1585.
- Herrick, F. W. (1984). Process for preparing microfibrillated cellulose. *United States Patent*, Pat. No. 4 481 077.
- Hsieh, Y. C., Yano, H., Nogi, M., & Eichhorn, S. J. (2008). An estimation of the Young's modulus of bacterial cellulose filaments. *Cellulose*, 15, 507–513.
- Hubbe, M. A., Rojas, O. J., Lucia, L. A., & Sain, M. (2008). Cellulosic nanocomposites: A review. *Bioresources*, 3, 929–980.
- Iwamoto, S., Nakagaito, A. N., & Yano, H. (2007). Nano-fibrillation of pulp fibers for the processing of transparent nanocomposites. *Applied Physics A – Materials Science & Processing*, 89, 461–466.
- Iwatake, A., Nogi, M., & Yano, H. (2008). Cellulose nanofiber-reinforced polylactic acid. *Composites Science and Technology*, 68, 2103–2106.
- Lapierre, L., Bouchard, J., & Berry, R. (2006). On the relationship between fibre length, cellulose chain length and pulp viscosity of a softwood sulfite pulp. *Holzforschung*, 60, 372–377.
- Leitner, J., Hinterstoisser, B., Wastyn, M., Keckes, J., & Gindl, W. (2007). Sugar beet cellulose nanofibril-reinforced composites. *Cellulose*, 14, 419–425.
- Mathew, A. P., Chakraborty, A., Oksman, K., & Sain, M. (2006). The structure and mechanical properties of cellulose nanocomposites prepared by twin screw extrusion. In K. Oksman & M. Sain (Eds.). *Cellulose nanocomposites: Processing, characterization, and properties* (Vol. 938, pp. 114–131). Washington, US: American Chemical Society.
- Nakagaito, A. N., & Yano, H. (2004). The effect of morphological changes from pulp fiber towards nanoscale fibrillated cellulose on the mechanical properties of high-strength plant fiber based composites. *Applied Physics A – Materials Science & Processing*, 78, 547–552.
- Nakagaito, A. N., & Yano, H. (2005). Novel high-strength biocomposites based on microfibrillated cellulose having nano-order-unit web-like network structure. *Applied Physics A – Materials Science & Processing*, 80, 155–159.
- Pandey, J. K., Kumar, A. P., Misra, M., Mohanty, A. K., Drzal, L. T., & Singh, R. P. (2005). Recent advances in biodegradable nanocomposites. *Journal of Nanoscience and Nanotechnology*, 5, 497–526.
- Panthapulakkal, S., Zerehschian, A., & Sain, M. (2005). Preparation and characterization of wheat straw fibers for reinforcing application in injection molded thermoplastic composites. *Bioresource Technology*, 97, 265–272.
- Sakurada, I., Nukushina, Y., & Ito, T. (1962). Experimental determination of the elastic modulus of crystalline regions in oriented polymers. *Journal of Polymer Science*, 57, 651–660.
- Spurr, A. R. (1969). A low-viscosity epoxy resin embedding medium for electron microscopy. *Journal of Ultrastructural Research*, 26, 31–43.
- Tashiro, K., & Kobayashi, M. (1991). Theoretical evaluation of 3-dimensional elastic-constants of native and regenerated celluloses – Role of hydrogen-bonds. *Polymer*, 32, 1516–1530.
- Turbak, A. F., Snyder, F. W., & Sandberg, J. (1983). Microfibrillated cellulose, a new cellulose product: Properties, uses and commercial potential. *Journal of Applied Polymer Science*, 37, 815–827.
- Uremovic, A., Dokk Glawischnig, T., Schuseil, J., Saake, B., Borchmann, A., Herrmann, A., et al. (1994). Chromatographische Untersuchungen zur quantitativen Bestimmung der Holzzucker. *Holz als Roh und Werkstoff*, 52, 347–354.
- Wan, W. K., Hutter, J. L., Millon, L., & Guhados, G. (2006). Bacterial cellulose and its nanocomposites for biomedical applications. In K. Oksman & M. Sain (Eds.). *Cellulose nanocomposites: Processing, characterization, and properties* (Vol. 938, pp. 221–241). Washington, US: American Chemical Society.
- Yano, H., Sugiyama, J., Nakagaito, A. N., Nogi, M., Matsuura, T., Hikita, M., et al. (2005). Optically transparent composites reinforced with networks of bacterial nanofibers. *Advanced Materials*, 17, 153–155.
- Zimmermann, T., Pöhler, E., & Geiger, T. (2004). Cellulose fibrils for polymer reinforcement. *Advanced Engineering Materials*, 6, 754–761.
- Zimmermann, T., Pöhler, E., & Schwaller, P. (2005). Mechanical and morphological properties of cellulose fibril reinforced nanocomposites. *Advanced Engineering Materials*, 7, 1156–1161.